HiMoE: Heterogeneity-Informed Mixture-of-Experts for Fair Spatial-Temporal Forecasting

Shaohan Yu¹, Pan Deng^{1*}, Yu Zhao¹, Junting Liu¹ and Zi'ang Wang¹

¹Beihang University

{doublepi,pandeng,iyzhao,liujunting,wangziang}@buaa.edu.cn

Abstract

Achieving fair prediction performance across nodes is crucial in the spatial-temporal domain, as it ensures the validity and reliability of forecasting outcomes. However, existing models focus primarily on improving the overall accuracy of the prediction, often neglecting the goal of achieving uniformity in the predictions. This task becomes particularly challenging due to the inherent spatial-temporal heterogeneity of the nodes. To address this issue, we propose a novel Heterogeneityinformed Mixture-of-Experts (HiMoE) for fair spatial-temporal forecasting. In particular, we design the Heterogeneity-Informed Graph Convolutional Network (HiGCN), which leverages the fusion of multi-graph and edge masking to flexibly model spatial dependencies. Moreover, we introduce the Node-wise Mixture-of-Experts (NMoE), which allocates prediction tasks of different nodes to suitable experts through graph decoupling routing. To further improve the model, fairness-aware loss and evaluation functions are proposed, optimizing the model with fairness and accuracy as objectives. Experiments on four datasets from different real-world scenarios demonstrate that HiMoE achieves the state-of-the-art performance, outperforming the best baseline with at lease 9.22% in all metrics.

1 Introduction

Spatial-temporal forecasting is a complex multi-objective prediction task, widely applied in fields such as transportation [Han et al., 2021b; Zheng et al., 2020; Choi et al., 2022; Deng et al., 2023; Lv et al., 2020; Zhao et al., 2023], climate [Wang et al., 2020; Qi et al., 2019; Jin et al., 2023b; Han et al., 2021a; Han et al., 2022], and other domains. Ensuring high prediction accuracy at each spatial node is a prerequisite for reliable and usable data predictions. However, existing models evaluate performance solely based on overall performance, overlooking differences in prediction accuracy

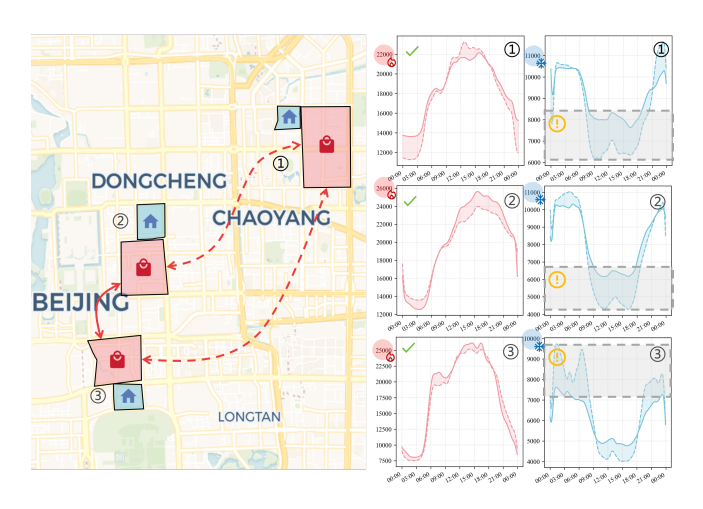


Figure 1: The diurnal variations in population across six regions of Beijing. The dashed curve represents the predicted values, while the solid curve represents the actual values. In each subplot, the MAE between the two curves is approximately 1000.

between different nodes [He et al., 2024]. In traffic prediction systems, poor prediction performance at specific nodes can lead to missed detection of traffic congestion, which may result in localized traffic paralysis. Achieving both accuracy and uniformity as objectives thus becomes a core challenge in spatial-temporal forecasting tasks.

However, the heterogeneity of spatial-temporal data poses a significant barrier to achieving fair predictions. Firstly, functional heterogeneity complicates accurate predictions. As illustrated in Figure 1, different areas in an urban grid may exhibit distinct characteristics. For example, residential areas (blue grids) tend to show lower populations during midday and higher populations during morning and evening hours, while commercial areas (red grids) typically exhibit the opposite pattern. Modeling relationships between regions with such functional differences becomes especially challenging, making it difficult to predict population dynamics across all areas. Secondly, data feature heterogeneity poses a challenge to achieving uniformity in the predictions. As shown in Figure 1, residential areas generally have a lower average population compared to commercial areas. When predicting across multiple areas, the same prediction error values correspond to different error ratios in these regions. For example, if the

^{*}Corresponding author.

model makes identical prediction error values for both residential and commercial areas, the error ratio in residential areas will be higher (because the prediction performance within the gray dashed box in the chart for residential areas is noticeably worse). Since the error ratio reflects the model's predictive capability, optimizing the model solely based on the mean error value would lead to worse prediction performance in residential areas and better performance in commercial areas. Therefore, most existing approaches that focus solely on improving the overall performance of prediction error values lead to biased outcomes. As a result, achieving fair predictions is both crucial and challenging.

Based on the previous discussion, the challenges posed by spatial-temporal data heterogeneity in forecasting tasks can be summarized as follows: (1) How to model spatial dependencies more flexibly to account for functional heterogeneity. (2) How to adapt existing training methods to mitigate biases in response to data feature heterogeneity. (3) How to effectively balance the multiobjective nature of spatial-temporal forecasting tasks, ensuring both accuracy and fairness.

In response to the above challenges, this paper proposes the following methods: (1) We propose Heterogeneity-Informed Graph Convolutional Network (HiGCN) as a key component of the expert model, leveraging multi-graph fusion and edge-level gating to model dependencies in functionally heterogeneous nodes. (2) We designed Weighted Absolute Error (WAE) and Standard Absolute Ratio Error (SARE) for the loss and evaluation functions to adapt to data feature heterogeneity, thus improving the uniformity of prediction results. (3) We present Node-wise Mixture-of-Experts (NMoE), based on fine-grained MoE. The model utilizes different experts to handle nodes with heterogeneous data features, with each expert addressing nodes with functional heterogeneity, thereby balancing the goals of accuracy and uniformity.

To the best of our knowledge, HiMoE is the first method to identify node-level bias in spatial-temporal predictions arising from existing training strategies and propose corresponding correction methods. Our contributions are as follows:

- We propose HiGCN as an integral component of experts and NMoE to manage experts, collaboratively enhancing HiMoE's ability to make fair predictions.
- We propose WAE and SARE to evaluate node-level prediction ratio errors by incorporating the heterogeneous data distribution as the model's inductive bias.
- Extensive experiments conducted on four urban computing datasets show that HiMoE consistently achieves state-of-the-art performance, significantly enhancing predictive accuracy and fairness across diverse scenarios, with improvements ranging from 9.22% to 55.71% across all metrics.

2 Related Work

2.1 Spatial-Temporal Data Forecasting

Spatial-temporal graph neural networks (STGNNs) have proven to be effective in modeling intricate relationships within spatial-temporal data [Jin *et al.*, 2023a]. Traditional

models establish robust baseline models by leveraging a variety of temporal and spatial modeling techniques [Han et al., 2021b; Choi et al., 2022; Deng et al., 2023; Song et al., 2020; Bai et al., 2020]. In contrast, contemporary approaches focus on harnessing innovative learning methods to fully exploit the untapped potential of existing models [Gao et al., 2024; Jiang et al., 2023; Ji et al., 2023; Dong et al., 2024; Chen et al., 2021].

Nevertheless, these models rarely recognize the multiobjective nature of spatial-temporal forecasting tasks. They often focus solely on improving overall predictive performance, neglecting fairness at the node level. Some models recognize the importance of fairness in spatial-temporal forecasting [Yan and Howe, 2019; Song *et al.*, 2023]. FairFor addresses this issue by generating group-relevant and groupirrelevant representations through adversarial learning [He *et al.*, 2024]. STMoE, on the other hand, leverages spatialtemporal representation learning to capture the unique patterns of each node and employs different experts to handle these distinct patterns, thus ensuring more balanced predictions in spatial-temporal forecasting [Li *et al.*, 2023]. However, using unbiased loss for achieving fair predictions remains an unexplored area.

2.2 Mixture of Experts

The Mixture of Experts (MoE) model, proposed by Shazeer et al. [Shazeer et al., 2016], is a machine learning framework designed to improve overall performance and efficiency by combining the complementary capabilities of multiple expert models. This architecture dynamically assigns the input data to specialized experts according to the characteristics of the task, allowing the model to achieve exceptional results in complex and diverse tasks [Cai et al., 2024]. MoE has seen extensive application in a variety of fields, such as Large Language Model (LLM) [Artetxe et al., 2022; Xue et al., 2025; Du et al., 2022] and image recognition [Riquelme et al., 2021; Theis and Bethge, 2015; Fan et al., 2022]. Recently, DeepSeek has demonstrated the potential of fine-grained Mixture-of-Experts (MoE) to develop robust language models, making a substantial impact in the field [Liu et al., 2024].

MoE has also been widely applied in spatial-temporal fore-casting across various domains. Wu et al. [Wu et al., 2024] utilized MoE to model different types of crime, capturing unique and shared patterns for collective multi-type crime prediction. Jiang et al. [Jiang et al., 2024] applied MoE to the prediction of real-world congestion, enhancing the accuracy in dynamic environments. Lee et al. [Lee and Ko, 2024] propose TESTAM, which employs experts with different spatio-temporal modeling approaches to capture both recurring and nonrecurring traffic patterns, achieving accurate spatio-temporal forecasting. However, these models often use a limited number of experts, failing to fully leverage the powerful modeling capabilities of fine-grained MoE, resulting in suboptimal performance.

3 Preliminary

At each time t, spatial-temporal data is represented as $X_t \in \mathbb{R}^N$, where N is the total number of nodes. We denote spatial-

temporal data from the time step m to the time step n across all nodes as $\mathbf{X}_{m:n} \in \mathbb{R}^{N \times (n-m+1)}$. The spatial-temporal graph at time t is expressed as $\mathcal{G} = (V, E, A)$, where V is the set of N nodes, E is the set of edges connecting nodes within V, and A is the adjacency matrix at time t. The problem is defined as follows:

Spatial-Temporal Data Forecasting. Given a graph $\mathcal G$ and spatial-temporal data from the previous T time steps, the goal is to learn a mapping function f to forecast spatial-temporal data for the next T' time steps. This mapping can be formally defined as:

$$\hat{\mathbf{X}}_{t+1:t+T'} = f(\mathbf{X}_{t-T+1:t}, \mathcal{G}). \tag{1}$$

Spatial-Temporal Fairness Criterion. Given the entire historical spatial-temporal dataset $\mathbf{X} \in \mathbb{R}^{N \times T}$, the mean characteristic of each node i is represented by $c_i = \text{mean}(\mathbf{X}^i)$. The Mean Absolute Error (MAE) for each node i is denoted by $e_i = \frac{1}{T'} \sum_{j=1}^{T'} |X_j^i - \hat{X}_j^i|$. To isolate spatial heterogeneity and mitigate the impact of temporal variation, we define the node-level ratio error as $r^i = e^i/c^i$. To assess the uniformity of node performance, we calculate the standard deviation of node-level ratio errors. The Standard Absolute Ratio Error (SARE) is a metric specifically designed to measure the consistency of predictions across nodes. A lower SARE value indicates greater uniformity in model performance:

$$SARE = std (\mathbf{r} \cdot mean(\mathbf{X})). \tag{2}$$

Here, $\mathbf{r} \in \mathbb{R}^N$ represents the vector of node-level ratio errors across all nodes, and multiplying by mean(\mathbf{X}) restores the data's original scale, allowing SARE to capture the variation in the model's predictive accuracy across diverse spatial regions.

4 Methodology

This section provides a detailed description of the HiMoE framework, as illustrated in Figure 2.

4.1 HiGCN: Heterogeneity-Informed Graph Convolutional Network

We design HiGCN as a key component within the expert model to address functional heterogeneity. Specifically, we construct a spatial-temporal graph learning module by integrating dynamic and static graphs, combined with a gating mechanism. This module enhances the representational capability of GCN through flexible spatial modeling.

The spatial-temporal graph learning module requires both static and dynamic graph inputs. The static graph A_s is directly derived from the distances between nodes, while the dynamic graph A_d is constructed by calculating the similarity based on the embedded spatial-temporal data $E_{t:t+T}$, as shown in the following formula:

$$A_d = \text{SoftMax}(E_{t:t+T}^T E_{t:t+T} - \text{diag}(E_{t:t+T}^T E_{t:t+T})).$$
 (3)

The removal of the diagonal elements before applying the softmax function is intended to emphasize the similarity between different nodes.

To uncover the latent relationships between nodes, we first use an encoding layer to learn the representations of node relationships, then apply a decoding layer to compute the corresponding relationship values based on these representations. Finally, a gating layer is used to filter out spurious connections and model the strengths of positive and negative correlations.:

$$A_f = \text{MLP}(A_d||A_s) \odot \tanh(W_a). \tag{4}$$

In Equation 4, $(A_d||A_s) \in \mathbb{R}^{N \times N \times 2}$ represents the concatenation operation, \odot signifies the Hadamard product, and $W_a \in \mathbb{R}^{N \times N}$ is a learnable parameter. The tanh function normalizes W_a within the range (-1,1), allowing the GCN greater control over extracting graph information.

To enable a finer-grained mixture of experts, the complexity of the expert models must be kept low. To improve efficiency, we utilize a GCN that formulates its layer-by-layer propagation based on a first-order approximation of localized spectral filters on the graph [Kipf and Welling, 2016]:

$$h^{l+1} = \sigma(A^l h^l W_1^l + I h^l W_2^l), \tag{5}$$

where l denotes the layer number of the GNN, and $A^l = A_f^l + (A_f^l)^T$ represents the adjacency matrix learned at the l-th GCN layer. Summing A_f^l and its transpose ensures matrix symmetry. Here, $h^l \in \mathbb{R}^{N \times C^l}$ serves as the input to the l-th layer, and $h^{l+1} \in \mathbb{R}^{N \times C^{l+1}}$ is the output of the l-th layer, where C denotes the number of channels. Additionally, W_1^l and W_2^l are learnable parameters, σ is the activation function, and I represents the identity matrix.

4.2 NMoE: Node-wise Mixture-of-Experts

To address data feature heterogeneity, we designed NMoE to assign different experts to nodes with varying data features. Specifically, our model decouples the spatial-temporal data into node-level time series, with each node's prediction task being handled by all experts, each of which operates on different subgraphs. The output is dominated by the experts that are better specialized in handling that particular node.

Decoupled Graph Routing Network

In the NMoE architecture, different experts are responsible for processing different types of nodes. Each expert receives the same spatial-temporal data but operates on distinct spatial-temporal graph structures. This design enables each expert to focus on specific groups of nodes with homogeneous data features, thereby enhancing prediction accuracy for each group while preserving global information. To ensure that nodes with data feature homogeneity are assigned to the same expert, we introduce a decoupled graph routing network to select edges corresponding to nodes of the respective type handled by each expert.

In this paper, we adopt the mean as the data feature. In a spatial-temporal graph, the dependency between nodes with heterogeneous means may lead to the propagation of errors. For example, even minor fluctuations in the input of high-mean nodes can significantly influence low-mean nodes through the GCN. Consequently, experts assigned to low-mean features should refrain from modeling relationships

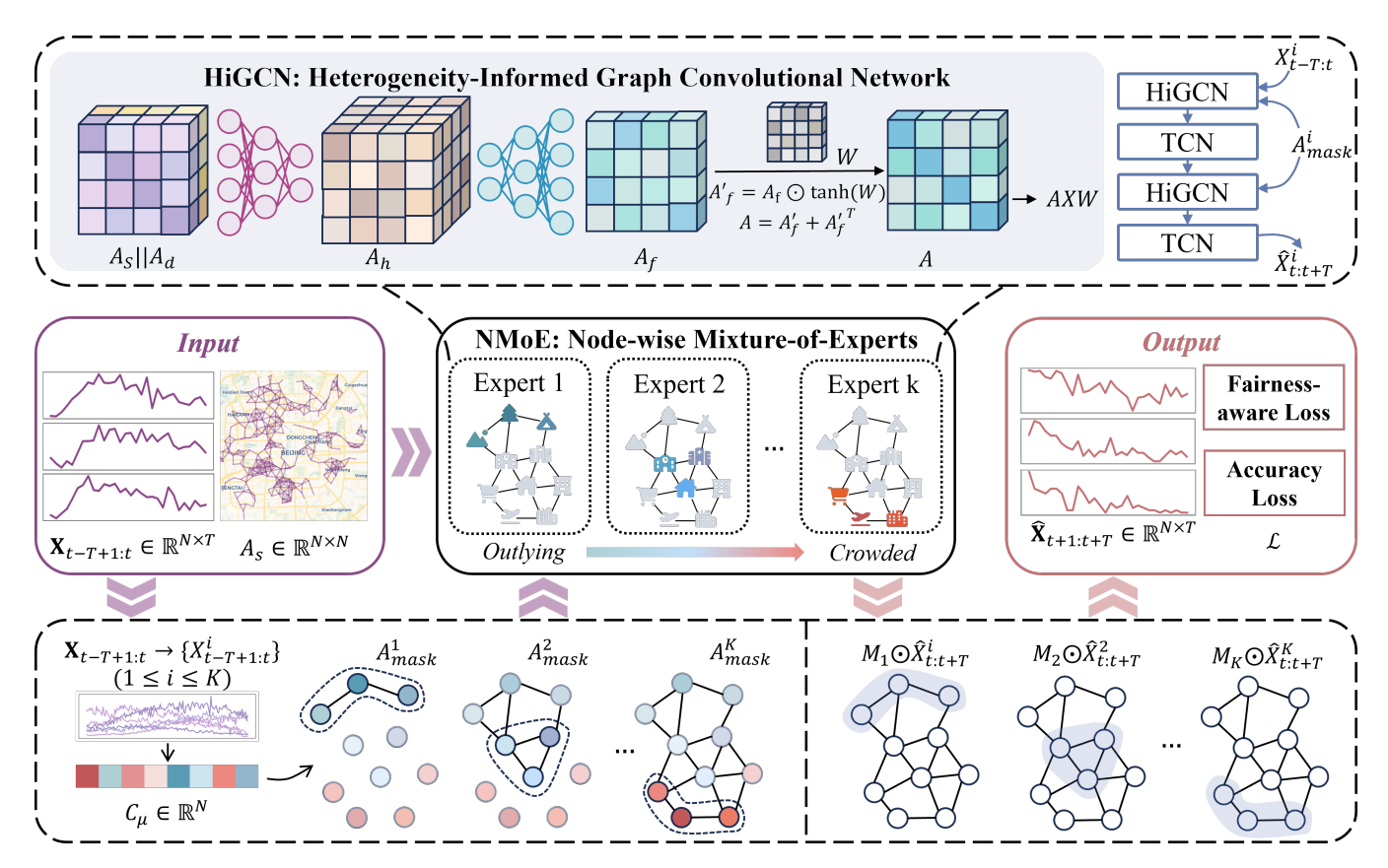


Figure 2: The overall architecture of the HiMoE model. The solid boxes represent the model pipeline, while the dashed boxes illustrate how the Mixture of Experts operates and outline the structure of the expert models.

with high-mean nodes, whereas experts for high-mean features can model relationships with any type of node.

To cluster nodes based on data feature homogeneity, we first compute the node-level mean of the input data $X_{t-T:t}$ as $C_{\mu} \in \mathbb{R}^{N}$, followed by z-score normalization of the mean features:

$$Z_{\mu} = \frac{(C_{\mu} - \operatorname{mean}(C_{\mu}))}{\operatorname{std}(C_{\mu})}.$$
 (6)

Next, we use $w_{i,i+1}$ as thresholds to decouple nodes with data feature heterogeneity. The value of $w_{i,i+1}$ is computed from learnable parameters as follows: For the first threshold, we set $w_{1,2}=\theta_1$, and for $2\leq i\leq k-1$, we recursively perform the calculation:

$$w_{i,i+1} = w_{i-1,i} + \text{ReLU}(\theta_i), \tag{7}$$

where ReLU ensures non-negativity, thus guaranteeing that w_{i+1} forms a monotonically increasing sequence. Using these thresholds, we classify the j-th node as belonging to the i-th expert if its value Z^j_μ satisfies the condition $w_i \leq Z^j_\mu \leq w_{i+1}$.

To generate adjacency matrices suitable for the different expert models, we need to consider that low-mean nodes are more susceptible to the influence of high-mean nodes, while high-mean nodes are less affected by low-mean nodes. Based on this assumption, we define the adjacency matrix mask for the i-th expert as:

$$A_{mask}^{i} = \sigma(\gamma \cdot (w_{i,i+1} - Z_{\mu}))^{T} \cdot \sigma(\gamma \cdot (w_{i,i+1} - Z_{\mu})).$$
(8)

In the above equation, σ means the sigmoid function. We first compute the probability $\sigma(\gamma \cdot (w_{i,i+1} - Z_\mu))$, which represents the likelihood that each node should be assigned to the i-th expert. The hyperparameter γ is a scaling factor that controls the strength of the soft margin classification. We then use this probability to construct the adjacency matrix mask A^i_{mask} . This mask filters out irrelevant information by multiplying it with the adjacency matrix when the expert model processes the spatial-temporal graph. The value of i ranges from 1 to k-1, where the k-th expert does not require a mask. The calculation of the adjacency matrix mask is illustrated in Figure 2, which provides a visual overview of the process.

Output Gating

We adopt a dense MoE strategy, activating all experts simultaneously for each node's prediction. If we were to apply the sparse MoE approach commonly used in LLMs to our model, each expert would only handle a small subset of nodes [Shazeer *et al.*, 2016]. However, when the GCN models the relationships between the nodes assigned to experts and those not assigned, it may impact prediction accuracy, as experts perform poorly on the nodes they do not handle. To effectively incorporate gating mechanisms in dense MoE, we con-

catenate the outputs of all experts as follows:

$$\hat{\mathbf{X}}_{t:t+T}^{\text{concat}} = \hat{\mathbf{X}}_{t:t+T}^{1} \parallel \hat{\mathbf{X}}_{t:t+T}^{2} \parallel \dots \parallel \hat{\mathbf{X}}_{t:t+T}^{k}, \qquad (9)$$

where $\hat{\mathbf{X}}_{t:t+T}^{\text{concat}} \in \mathbb{R}^{k \times N \times T'}$. Using a learnable gating matrix, we select the output of the expert model corresponding to each node:

$$\hat{\mathbf{X}}_{t:t+T} = \operatorname{sum}(\hat{\mathbf{X}}_{t:t+T}^{\text{concat}} \odot \operatorname{sigmoid}(W_o)), \tag{10}$$

where $W_o \in \mathbb{R}^{k \times N}$ is a learnable output gating matrix, and the sigmoid operation is applied to each expert for every node, enabling HiMoE to dynamically adjust the weights assigned to the outputs of different expert model.

4.3 Fairness-Aware Loss Functions and Metrics

Due to the node-level biases present in existing loss functions and evaluation metrics, we need to design an unbiased loss function and evaluation metric. In this design, prediction accuracy and prediction uniformity must be treated with equal importance. The loss function should account for accuracy and uniformity simultaneously. As for the evaluation metrics, there should be accuracy-based, uniformity-based, and combined accuracy-uniformity measures.

To assess the magnitude of errors during the prediction process while capturing differences in node-level errors, we propose a weighted approach to the loss function. When calculating Equation 2, we adopt a node-level proportional error c_i . After recovering the data features of c_i , it can be used to weight the loss:

WAE =
$$\sum_{i=1}^{N} \frac{mean(X)}{c_i} \sum_{t=1}^{T'} |\hat{x}_t^i - x_t^i|.$$
 (11)

It is crucial to address potential data leakage when calculating the feature c_i and $\operatorname{mean}(X)$. Specifically, for the loss function, only the training and validation sets should be utilized in the computation. In contrast, the evaluation metric should be computed using the complete dataset to ensure an accurate assessment. As we have previously defined an evaluation strategy for the consistency of prediction results, we utilize both SARE and WAE as the loss function:

$$\mathcal{L}(X, \hat{X}) = \alpha \mathcal{L}_{WAE}(X, \hat{X}) + \beta \mathcal{L}_{SARE}(X, \hat{X}), \quad (12)$$

where α and β are hyperparameters. Additionally, WAE and SARE are also incorporated as new components of our evaluation metrics.

5 Experiment

5.1 Experimental Setup

Data Descriptions

We conducted experiments on four datasets: PeMS04, KnowAir, Beijing, and Tongzhou. The PeMS04 dataset is derived from the Caltrans Performance Measurement System (PeMS), a widely used public dataset [Guo et al., 2019]. This study utilizes only the traffic flow data from PeMS04. KnowAir covers a broad geographical area for PM2.5 forecasting, including several heavily polluted regions across China [Wang et al., 2020]. The Tongzhou and Beijing

datasets, collected by China Mobile, include road segment speed data for Tongzhou district and real-time population data for urban grids in Beijing. In summary, our datasets encompass various types of data collected across multiple spatial scales, demonstrating their diversity and wide coverage. We apply Z-score normalization to normalize the data. After that, We split the datasets into training, validation, and test data using the ratio of 6:2:2. The detailed information for the four datasets is described in Table 1.

Table 1: Detailed information of the four datasets

Dataset	Sensors	Time Steps	Time Interval
PEMS04	307	5 min	16992
KnowAir	184	60 min	11688
Beijing	500	5 min	26784
Tongzhou	645	5 min	25056

Baselines

We compare HiMoE with the following baselines: (1) **Graph** WaveNet [Wu et al., 2019] uses an adaptive adjacency matrix to capture spatial dependencies and combines graph convolution with dilated causal convolution for joint modeling of spatial and temporal dependencies. (2) **ASTGCN** [Guo et al., 2019] employs a spatial-temporal attention mechanism and convolution module to learn dynamic correlations. (3) MTGNN [Wu et al., 2020] applies a graph-based GNN approach to model multivariate time series, handling scenarios with or without a predefined graph structure. (4) **D2STGNN** [Shao et al., 2022] integrates dynamic graph learning for spatial dependency modeling and uses both diffusion and inherent models to capture hidden time series. (5) **TESTAM** [Lee and Ko, 2024] introduces a Mixture-of-Experts model with diverse graph architectures to enhance prediction accuracy. (6) **BigST** [Han et al., 2024] uses a linearized global spatial convolution network, reducing complexity for large-scale road network learning and message passing. (7) **STMoE** [Li et al., 2023] offers a model-agnostic framework to mitigate performance bias across road segments, ensuring more balanced predictions.

Evaluation Metrics

Based on previous studies, we use MAE, RMSE, and MAPE to evaluate accuracy. To assess fairness, we employ WAE and SARE, with WAE evaluating both accuracy and fairness.

Implementation Details

We implemented our model and the baseline models using the PyTorch framework on the NVIDIA Tesla V100S GPU. For all datasets, we used the first 12 time steps T to predict the subsequent 12 time steps T'. The loss function for each baseline model followed its original definition. All models were trained using the Adam optimizer with 500 epochs. Our model was trained with a batch size of 64, a learning rate of 0.003, and a weight decay of 0.0001. For HiGCN, we set the hidden layer dimension of the MLP to 8, the hidden layer dimension of the graph convolution to 64, and used GELU

Table 2: The performance on PeMS04 Flow, Beijing Population, Tongzhou Speed, and KnowAir PM2.5 is presented, with the best and second-best performances in each dataset and metrics are bolded and underlined.

Dataset	Metric	GWNet	ASTGCN	MTGNN	D2STGNN	TESTAM	BigST	STMoE	HiMoE
PeMS04	MAE	18.02	16.80	17.22	19.24	18.67	17.99	17.68	12.36
	RMSE	29.32	27.40	28.33	31.06	30.44	29.53	28.83	18.45
	MAPE	12.97	11.89	12.17	14.17	12.99	12.95	12.39	10.00
	WAE	15.12	14.12	14.40	16.17	15.56	14.65	14.83	10.07
	SARE	22.90	<u>21.42</u>	22.07	24.38	23.56	22.36	22.53	12.24
Beijing	MAE	100.93	144.41	90.02	153.70	136.74	119.93	94.64	60.44
	RMSE	349.49	513.95	296.99	449.57	368.61	423.81	356.39	132.71
	MAPE	17.83	45.19	<u>17.10</u>	22.87	21.51	28.29	36.35	14.97
	WAE	80.10	111.64	<u>71.71</u>	125.27	117.60	95.46	75.07	46.02
	SARE	370.65	532.21	319.48	473.56	434.07	442.01	399.39	127.77
Tongzhou	MAE	3.02	2.95	2.94	3.07	3.10	3.12	2.93	2.66
	RMSE	4.70	4.54	4.59	4.72	4.74	4.75	4.58	3.86
	MAPE	8.90	8.57	8.57	9.05	9.06	9.26	8.57	7.42
	WAE	2.88	2.81	2.80	2.93	2.98	2.98	2.80	2.53
	SARE	3.52	<u>3.39</u>	3.46	3.50	3.51	3.49	3.46	2.75
KnowAir	MAE	16.77	18.33	16.18	19.29	23.61	19.71	16.08	8.64
	RMSE	27.26	30.01	26.22	31.04	38.18	31.69	25.92	12.67
	MAPE	39.21	45.30	38.58	48.66	60.59	48.64	39.30	22.54
	WAE	15.93	17.30	15.36	18.27	22.18	18.62	<u>15.30</u>	8.17
	SARE	21.31	23.07	20.41	23.67	27.90	24.07	20.23	8.96

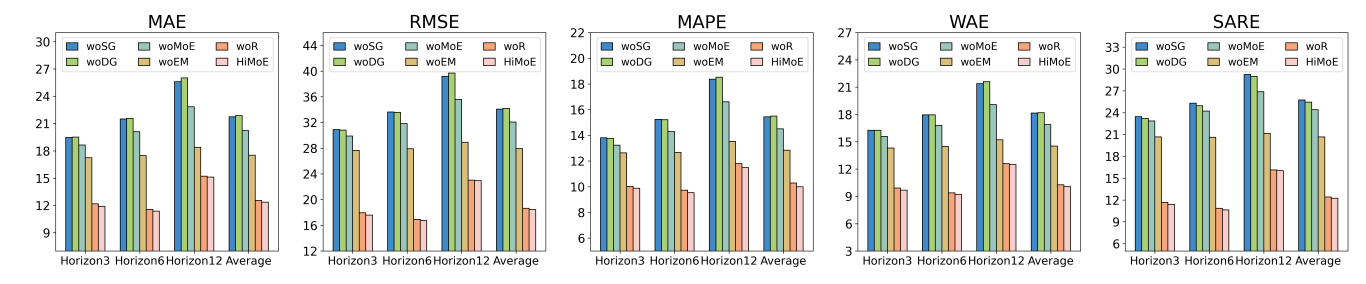


Figure 3: Ablation Study on PeMS04

as the activation function. For NMoE, we set the number of experts to 14 for all datasets. For the fairness-aware loss function, we set α to 1 and β to 0.5. For more detailed implementation information, readers can refer to our public code repository.

5.2 Performance Comparision

According to Table 2, HiMoE outperforms other baselines across datasets with diverse data types and spatial scopes, demonstrating its adaptability to various real-world scenarios. Specifically, on the PeMS04 dataset, our model achieves improvements of 26.43%, 32.66%, 15.90%, 28.68%, and 43.47% over the best baseline (ASTGCN [Guo *et al.*, 2019]) in MAE, RMSE, MAPE, WAE, and SARE, respectively. Similarly, on the Beijing dataset, it achieves gains of 32.86%, 55.31%, 12.46%, 35.83%, and 60.01%. Additionally, HiMoE delivers improvements of 9.22%, 14.98%, 13.42%, 9.64%, and 18.88% on the Tongzhou dataset, and achieves notable progress of 46.27%, 51.12%, 41.58%, 46.60%, and 55.71% on the KnowAir dataset.

Compared with models specifically designed for traf-

fic prediction (e.g., GraphWaveNet [Wu et al., 2019], D2STGNN [Shao et al., 2022], BigST [Han et al., 2024]), our model exhibits superior performance on the Beijing and KnowAir datasets, emphasizing HiMoE's scalability across diverse scenarios. Similarly, relative to fully self-learning graph models (e.g., MTGNN [Wu et al., 2020]), our model's results validate that learning dynamic and static graphs is more effective for capturing spatial-temporal dependencies. In contrast to MoE-based approaches (e.g., TESTAM [Lee and Ko, 2024]), the performance of our model highlights the fine-grained MoE structure and NMoE design. Furthermore, against existing fair prediction models (e.g., STMoE [Li et al., 2023]), our model demonstrates significant advantages in fairness evaluation metrics, showcasing the importance of the synergy between model architecture and training strategy in spatial-temporal prediction tasks. Nevertheless, the final performance of any model is subject to various influencing factors. Therefore, although HiMoE achieves outstanding results as presented in Table 2, these results alone do not comprehensively reflect the effectiveness of each method.

Table 3: The overall performance on the PeMS04 Flow dataset is shown, with all models trained using the fairness-focused loss function. The best and second-best performances in each dataset and metric are bolded and underlined.

Model	MAE	RMSE	MAPE	WAE	SARE
GWNet	18.34	29.31	12.90	15.26	22.07
ASTGCN	16.86	26.88	12.12	14.05	20.20
MTGNN	17.43	28.11	12.51	14.50	21.20
D2STGNN	19.48	31.04	14.14	16.24	23.55
TESTAM	27.06	41.40	19.42	22.55	30.85
BigST	18.05	29.24	13.21	15.03	22.32
STMoE	18.00	28.86	12.73	14.96	21.72
HiMoE	12.36	18.45	10.00	10.07	12.24

5.3 Ablation Studies

In this section, we conduct an ablation study on the PeMS04 dataset to evaluate the effectiveness of each submodule. Five variants of the model are compared: (1) woSG: By replacing the learnable adjacency matrix with a dynamic one, the influence of the static adjacency matrix on the model is removed. (2) woDG: By substituting the learnable adjacency matrix with a static one, the effect of the dynamic adjacency matrix on the model is eliminated. (3) woEM: The tanh mask applied to the edges in each HiGCN module is removed. (4) woMoE: The MoE structure is removed, leaving only a single expert for predictions. (5) woR: Removes the decoupled graph routing network, distinguishing experts solely through output gating. The prediction results are shown in Figure 3.

First, replacing the learnable graph with a dynamic or static graph leads to significant performance degradation, demonstrating the necessity of graph learnability. Second, we find that removing the edge mask leads to a decline in prediction accuracy, demonstrating that this mask is indispensable in modeling dependencies. Third, using a single expert model results in a significant performance gap compared to HiMoE, demonstrating that fine-grained MoE greatly enhances predictive capability. Moreover, when the decoupled graph routing is removed, the slight performance decline further supports the assumption that reducing the modeling of certain dependencies helps achieve more accurate predictions.

5.4 Loss Function Studies

Following the development of the fairness-focused loss function, it is crucial to examine whether other models can benefit from its application to achieve improved performance. In this section, we apply the fairness-focused loss function to train baseline models on the PeMS04 dataset. The performance of the models on PeMS04 is presented in Table 3.

First, some models, such as TESTAM, fail to train effectively with the fairness-focused loss function, resulting in performance degradation. Second, for most models (e.g., Graph WaveNet), there is minimal change in MAE, RMSE, MAPE, and WAE when using different loss functions. However, SARE decreases after training with the fairness-focused loss function. Moreover, HiMoE achieves significant improvements across most evaluation metrics when trained using Equation 12 as the loss function compared to using MAE

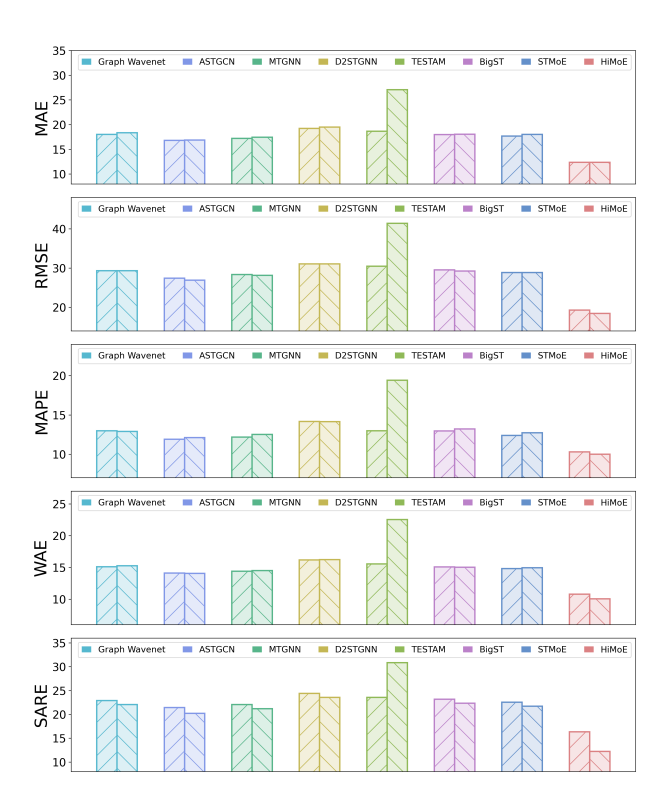


Figure 4: Comparison of baseline model performance with different loss functions: the left bar shows performance with MAE loss and the right bar with fairness-aware loss.

as the loss. Specifically, while there is no difference in MAE, we observed improvements of 4.35%, 3.00%, 6.59%, and 25.06% in RMSE, MAPE, WAE, and RWSE, respectively. In contrast, the improvements for other models were limited, with maximum gains of -0.36%, 1.90%, 0.54%, 0.50%, and 5.70% across these five metrics.

These findings suggest that simply guiding the model through the loss function may not be sufficient to achieve notable improvements in the uniformity of spatial-temporal prediction performance. HiMoE, by incorporating the NMoE design, is better aligned with the fairness loss function, leading to significant improvements in fairness metrics. Additionally, the uniformity evaluation metric strongly correlates with accuracy metrics. Trained with our proposed loss function, Hi-MoE consistently improves both fairness and prediction accuracy, demonstrating the effectiveness of the loss function in balancing these objectives.

6 Conclusion

This paper presents HiMoE, a fine-grained MoE-based framework for fair forecasting, designed to address the challenges of spatial and temporal heterogeneity. Specifically, we design HiGCN to address functional heterogeneity and NMoE to tackle data feature heterogeneity. Additionally, we propose loss and evaluation functions for the quantification of fairness. Extensive experiments demonstrate that our approach outperforms existing methods in both accuracy and fairness across various datasets.

References

- [Artetxe et al., 2022] Mikel Artetxe, Shruti Bhosale, Naman Goyal, Todor Mihaylov, Myle Ott, Sam Shleifer, Xi Victoria Lin, Jingfei Du, Srinivasan Iyer, Ramakanth Pasunuru, et al. Efficient large scale language modeling with mixtures of experts. In *Proceedings of the 2022 Conference on Empirical Methods in Natural Language Processing*, pages 11699–11732, 2022.
- [Bai et al., 2020] Lei Bai, Lina Yao, Can Li, Xianzhi Wang, and Can Wang. Adaptive graph convolutional recurrent network for traffic forecasting. Advances in neural information processing systems, 33:17804–17815, 2020.
- [Cai *et al.*, 2024] Weilin Cai, Juyong Jiang, Fan Wang, Jing Tang, Sunghun Kim, and Jiayi Huang. A survey on mixture of experts. *arXiv preprint arXiv:2407.06204*, 2024.
- [Chen et al., 2021] Xu Chen, Junshan Wang, and Kunqing Xie. Trafficstream: A streaming traffic flow forecasting framework based on graph neural networks and continual learning. Proceedings of the Thirtieth International Joint Conference on Artificial Intelligence, 2021.
- [Choi et al., 2022] Jeongwhan Choi, Hwangyong Choi, Jeehyun Hwang, and Noseong Park. Graph neural controlled differential equations for traffic forecasting. In *Proceedings of the AAAI conference on artificial intelligence*, volume 36, pages 6367–6374, 2022.
- [Deng et al., 2023] Pan Deng, Yu Zhao, Junting Liu, Xiaofeng Jia, and Mulan Wang. Spatio-temporal neural structural causal models for bike flow prediction. *Proceedings of the AAAI Conference on Artificial Intelligence*, 37(4):4242–4249, Jun. 2023.
- [Dong et al., 2024] Zheng Dong, Renhe Jiang, Haotian Gao, Hangchen Liu, Jinliang Deng, Qingsong Wen, and Xuan Song. Heterogeneity-informed meta-parameter learning for spatiotemporal time series forecasting. In *Proceedings of the 30th ACM SIGKDD Conference on Knowledge Discovery and Data Mining*, pages 631–641, 2024.
- [Du et al., 2022] Nan Du, Yanping Huang, Andrew M Dai, Simon Tong, Dmitry Lepikhin, Yuanzhong Xu, Maxim Krikun, Yanqi Zhou, Adams Wei Yu, Orhan Firat, et al. Glam: Efficient scaling of language models with mixtureof-experts. In *International Conference on Machine* Learning, pages 5547–5569. PMLR, 2022.
- [Fan et al., 2022] Zhiwen Fan, Rishov Sarkar, Ziyu Jiang, Tianlong Chen, Kai Zou, Yu Cheng, Cong Hao, Zhangyang Wang, et al. M³vit: Mixture-of-experts vision transformer for efficient multi-task learning with model-accelerator co-design. Advances in Neural Information Processing Systems, 35:28441–28457, 2022.
- [Gao et al., 2024] Haotian Gao, Renhe Jiang, Zheng Dong, Jinliang Deng, Yuxin Ma, and Xuan Song. Spatial-temporal-decoupled masked pre-training for spatiotemporal forecasting. In Kate Larson, editor, *Proceedings of the Thirty-Third International Joint Conference on Artificial Intelligence, IJCAI-24*, pages 3998–4006. International Joint Conferences on Artificial Intelligence Organization, 8 2024. Main Track.

- [Guo et al., 2019] Shengnan Guo, Youfang Lin, Ning Feng, Chao Song, and Huaiyu Wan. Attention based spatial-temporal graph convolutional networks for traffic flow forecasting. In *Proceedings of the AAAI conference on artificial intelligence*, volume 33, pages 922–929, 2019.
- [Han et al., 2021a] Jindong Han, Hao Liu, Hengshu Zhu, Hui Xiong, and Dejing Dou. Joint air quality and weather prediction based on multi-adversarial spatiotemporal networks. In *Proceedings of the AAAI Conference on Artificial Intelligence*, volume 35, pages 4081–4089, 2021.
- [Han et al., 2021b] Liangzhe Han, Bowen Du, Leilei Sun, Yanjie Fu, Yisheng Lv, and Hui Xiong. Dynamic and multi-faceted spatio-temporal deep learning for traffic speed forecasting. In Proceedings of the 27th ACM SIGKDD conference on knowledge discovery & data mining, pages 547–555, 2021.
- [Han *et al.*, 2022] Jindong Han, Hao Liu, Haoyi Xiong, and Jing Yang. Semi-supervised air quality forecasting via self-supervised hierarchical graph neural network. *IEEE Transactions on Knowledge and Data Engineering*, 35(5):5230–5243, 2022.
- [Han et al., 2024] Jindong Han, Weijia Zhang, Hao Liu, Tao Tao, Naiqiang Tan, and Hui Xiong. Bigst: Linear complexity spatio-temporal graph neural network for traffic forecasting on large-scale road networks. Proc. VLDB Endow., 17(5):1081–1090, May 2024.
- [He et al., 2024] Hui He, Qi Zhang, Shoujin Wang, Kun Yi, Zhendong Niu, and Longbing Cao. Learning informative representation for fairness-aware multivariate time-series forecasting: A group-based perspective. *IEEE Transactions on Knowledge and Data Engineering*, 36(6):2504–2516, 2024.
- [Ji et al., 2023] Jiahao Ji, Jingyuan Wang, Chao Huang, Junjie Wu, Boren Xu, Zhenhe Wu, Junbo Zhang, and Yu Zheng. Spatio-temporal self-supervised learning for traffic flow prediction. In *Proceedings of the AAAI con*ference on artificial intelligence, volume 37, pages 4356– 4364, 2023.
- [Jiang et al., 2023] Renhe Jiang, Zhaonan Wang, Jiawei Yong, Puneet Jeph, Quanjun Chen, Yasumasa Kobayashi, Xuan Song, Shintaro Fukushima, and Toyotaro Suzumura. Spatio-temporal meta-graph learning for traffic forecasting. In Proceedings of the AAAI Conference on Artificial Intelligence, volume 37, pages 8078–8086, 2023.
- [Jiang et al., 2024] Wenzhao Jiang, Jindong Han, Hao Liu, Tao Tao, Naiqiang Tan, and Hui Xiong. Interpretable cascading mixture-of-experts for urban traffic congestion prediction. In *Proceedings of the 30th ACM SIGKDD Conference on Knowledge Discovery and Data Mining*, pages 5206–5217, 2024.
- [Jin et al., 2023a] Guangyin Jin, Yuxuan Liang, Yuchen Fang, Zezhi Shao, Jincai Huang, Junbo Zhang, and Yu Zheng. Spatio-temporal graph neural networks for predictive learning in urban computing: A survey. *IEEE Trans. on Knowl. and Data Eng.*, 36(10):5388–5408, November 2023.

- [Jin et al., 2023b] Xue-Bo Jin, Zhong-Yao Wang, Jian-Lei Kong, Yu-Ting Bai, Ting-Li Su, Hui-Jun Ma, and Prasun Chakrabarti. Deep spatio-temporal graph network with self-optimization for air quality prediction. *Entropy*, 25(2):247, 2023.
- [Kipf and Welling, 2016] Thomas N Kipf and Max Welling. Semi-supervised classification with graph convolutional networks. *arXiv preprint arXiv:1609.02907*, 2016.
- [Lee and Ko, 2024] Hyunwook Lee and Sungahn Ko. TES-TAM: A time-enhanced spatio-temporal attention model with mixture of experts. In *The Twelfth International Conference on Learning Representations*, 2024.
- [Li et al., 2023] Shuhao Li, Yue Cui, Yan Zhao, Weidong Yang, Ruiyuan Zhang, and Xiaofang Zhou. St-moe: Spatio-temporal mixture-of-experts for debiasing in traffic prediction. In *Proceedings of the 32nd ACM International Conference on Information and Knowledge Management*, CIKM '23, page 1208–1217, New York, NY, USA, 2023. Association for Computing Machinery.
- [Liu et al., 2024] Aixin Liu, Bei Feng, Bing Xue, Bingxuan Wang, Bochao Wu, Chengda Lu, Chenggang Zhao, Chengqi Deng, Chenyu Zhang, Chong Ruan, et al. Deepseek-v3 technical report. arXiv preprint arXiv:2412.19437, 2024.
- [Lv et al., 2020] Mingqi Lv, Zhaoxiong Hong, Ling Chen, Tieming Chen, Tiantian Zhu, and Shouling Ji. Temporal multi-graph convolutional network for traffic flow prediction. IEEE Transactions on Intelligent Transportation Systems, 22(6):3337–3348, 2020.
- [Qi et al., 2019] Yanlin Qi, Qi Li, Hamed Karimian, and Di Liu. A hybrid model for spatiotemporal forecasting of pm2.5 based on graph convolutional neural network and long short-term memory. Science of The Total Environment, 664:1–10, 2019.
- [Riquelme et al., 2021] Carlos Riquelme, Joan Puigcerver, Basil Mustafa, Maxim Neumann, Rodolphe Jenatton, André Susano Pinto, Daniel Keysers, and Neil Houlsby. Scaling vision with sparse mixture of experts. Advances in Neural Information Processing Systems, 34:8583–8595, 2021.
- [Shao *et al.*, 2022] Zezhi Shao, Zhao Zhang, Wei Wei, Fei Wang, Yongjun Xu, Xin Cao, and Christian S. Jensen. Decoupled dynamic spatial-temporal graph neural network for traffic forecasting. *Proc. VLDB Endow.*, 15(11):2733–2746, July 2022.
- [Shazeer et al., 2016] Noam Shazeer, Azalia Mirhoseini, Krzysztof Maziarz, Andy Davis, Quoc Le, Geoffrey Hinton, and Jeff Dean. Outrageously large neural networks: The sparsely-gated mixture-of-experts layer. In *International Conference on Learning Representations*, 2016.
- [Song et al., 2020] Chao Song, Youfang Lin, Shengnan Guo, and Huaiyu Wan. Spatial-temporal synchronous graph convolutional networks: A new framework for spatialtemporal network data forecasting. In *Proceedings of* the AAAI conference on artificial intelligence, volume 34, pages 914–921, 2020.

- [Song et al., 2023] Zixing Song, Yuji Zhang, and Irwin King. Towards fair financial services for all: A temporal gnn approach for individual fairness on transaction networks. In *Proceedings of the 32nd ACM international conference on information and knowledge management*, pages 2331–2341, 2023.
- [Theis and Bethge, 2015] Lucas Theis and Matthias Bethge. Generative image modeling using spatial lstms. *Advances in neural information processing systems*, 28, 2015.
- [Wang et al., 2020] Shuo Wang, Yanran Li, Jiang Zhang, Qingye Meng, Lingwei Meng, and Fei Gao. Pm2.5-gnn: A domain knowledge enhanced graph neural network for pm2.5 forecasting. In Proceedings of the 28th International Conference on Advances in Geographic Information Systems, SIGSPATIAL '20, page 163–166, New York, NY, USA, 2020. Association for Computing Machinery.
- [Wu et al., 2019] Zonghan Wu, Shirui Pan, Guodong Long, Jing Jiang, and Chengqi Zhang. Graph wavenet for deep spatial-temporal graph modeling. In *Proceedings of the 28th International Joint Conference on Artificial Intelligence*, IJCAI'19, page 1907–1913. AAAI Press, 2019.
- [Wu et al., 2020] Zonghan Wu, Shirui Pan, Guodong Long, Jing Jiang, Xiaojun Chang, and Chengqi Zhang. Connecting the dots: Multivariate time series forecasting with graph neural networks. In Proceedings of the 26th ACM SIGKDD International Conference on Knowledge Discovery & Data Mining, KDD '20, page 753–763, New York, NY, USA, 2020. Association for Computing Machinery.
- [Wu et al., 2024] Ziyang Wu, Fan Liu, Jindong Han, Yuxuan Liang, and Hao Liu. Spatial-temporal mixture-of-graph-experts for multi-type crime prediction. arXiv preprint arXiv:2409.15764, 2024.
- [Xue et al., 2025] Fuzhao Xue, Zian Zheng, Yao Fu, Jinjie Ni, Zangwei Zheng, Wangchunshu Zhou, and Yang You. Openmoe: an early effort on open mixture-of-experts language models. In *Proceedings of the 41st International Conference on Machine Learning*, ICML'24. JMLR.org, 2025.
- [Yan and Howe, 2019] An Yan and Bill Howe. Fairst: Equitable spatial and temporal demand prediction for new mobility systems. In *Proceedings of the 27th ACM SIGSPATIAL International Conference on Advances in Geographic Information Systems*, pages 552–555, 2019.
- [Zhao et al., 2023] Yu Zhao, Pan Deng, Junting Liu, Xiaofeng Jia, and Mulan Wang. Causal conditional hidden markov model for multimodal traffic prediction. *Proceedings of the AAAI Conference on Artificial Intelligence*, 37(4):4929–4936, Jun. 2023.
- [Zheng et al., 2020] Chuanpan Zheng, Xiaoliang Fan, Cheng Wang, and Jianzhong Qi. Gman: A graph multi-attention network for traffic prediction. In *Proceedings of the AAAI conference on artificial intelligence*, volume 34, pages 1234–1241, 2020.